Available online at www.sciencedirect.com
SCIENCE DIRECT
Catalysis Today 102–103 (2005) 94–100
CATALYSIS TODAY
www.elsevier.com/locate/cattod

High-efficiency WO_3/carbon nanotubes for olefin skeletal isomerization

Barbara Pietruszka, François Di Gregorio, Nicolas Keller, Valérie Keller *

Laboratoire des Matériaux, Surface et Procédés pour la Catalyse, UMR 7515 CNRS and ELCASS (European Laboratory for Catalysis and Surface Sciences), Louis Pasteur University, 25, rue Becquerel BP 08, 67087 Strasbourg Cedex 2, France

Available online 19 March 2005

Abstract

WO_3/carbon nanotube (CNT) catalysts with different WO_3 loadings were prepared by wet impregnation with ammonium paratungstate as precursor, characterized by X-ray diffraction, temperature-programmed reduction, transmission electron microscopy and X-ray photoemission spectroscopy. These materials were tested for C_6 olefin skeletal isomerization in different activation (pre-reduction) conditions and compared to a reference tungstated zirconia, WO_3/ZrO_2, catalyst. They led to very high skeletal isomerization selectivities at 200 °C at high conversion level without any observable deactivation.

Keywords: Carbon nanotubes; Skeletal isomerization; Tungsten oxide reducibility; Nanowire; Film

1. Introduction

Solid acid catalysts play an important role in chemical and petroleum industries in hydrocarbon conversion reactions required in octane enhancement processes, such as cracking, isomerization and alkylation [1–3], which can form highly branched isoparaffins. Such reactions require strong or moderate acid catalysts. The detrimental environmental impact of halide-type solid acids led to develop halide-free catalysts, and tungsten oxides supported on oxide carriers have, thus, extensively been investigated as alternative catalysts for hydrocarbon isomerization processes due to the acidic character of supported tungsten oxide [4–10]. Among different oxide support materials, Al_2O_3 and ZrO_2 have been widely used as support for tungsten oxide but very few investigations on the use of carbon as support for hydrocarbon reforming reactions have been reported [11–13], despite the important role of carbon as a support [14]. It is now admitted that both active-phase-support interaction and tungsten content have a high influence on the activity of WO_3-reduced supported catalysts towards skeletal isomerization due to the extension of tungsten species reducibility [15,16].

Among the carbon materials, carbon nanotubes (CNTs) have attracted attention in the last decade in the field of catalysis because of potential applications as catalyst support and peculiar behaviors in terms of conversion or selectivity, which were attributed to specific active-phase-support interaction, limitation of mass transfer phenomena problems and/or to the existence of confinement effects inside CNTs [17].

Up to now, the use of CNTs as support in the field of heterogeneous catalysis remains mainly devoted to liquid-phase reactions using supported metals. The aim of this article is to report on the gas-phase use of WO_3/CNTs as catalyst for the 4-methyl-1-pentene (4M1Pen) isomerization. The catalysts will be characterized by X-ray diffraction (XRD), transmission electron microscopy (TEM), temperature-programmed reduction (TPR) and X-ray photoemission spectroscopy (XPS).

2. Experimental section

2.1. Catalyst preparation

Open multi-walled CNTs with inner and outer average diameters of 40 and 80 nm, respectively, and lengths up to about 200 μm were supplied by Appl. Sci. Inc. (OH, USA).

* Corresponding author. Tel.: +33 3 90 24 27 36; fax: 33 3 90 24 27 61.
E-mail address: vkeller@chimie.u-strasbg.fr (V. Keller).

0920-5861/$ – see front matter © 2005 Elsevier B.V. All rights reserved.
doi:10.1016/j.cattod.2005.02.014

They had a non-microporous specific surface area of 25 m^2/g obtained by BET measurement using N_2 at LN_2 temperature. Deposition of tungsten was performed by wet impregnation of the bare CNTs with an aqueous solution (20 mL) of ammonium metatungstate pentahydrate, $(NH_4)_{10}W_{12}O_{41}\cdot 5H_2O$, at pH close to 5. The CNTs were added to the precursor salt aqueous solution kept under vigorous stirring at 80 °C for 20 min before the slow evaporation of the solvent at room temperature. The resulting material was further dried overnight at 120 °C. The WO_3 content was taken at 4, 17 and 30 wt.% relative to the total weight of catalyst. The dried materials were finally calcinated at 350 °C for 2 h. Comparison was made with a WO_3 (25 wt.%)/ZrO_2 reference catalyst prepared following the same procedure and using commercially available monoclinic ZrO_2 supplied by Johnson Matthey [16]. Catalytic performances were reported in terms of specific rate of hydrocarbon transformation expressed in mol/s/(g of WO_3), isomerization selectivity and stability as a function of time.

2.2. Characterization techniques

Structural characterizations were done by powder XRD measurements on a Siemens Diffractometer Model D-5000, using Cu Kα radiation. The nature of the phase in the sample was checked using the database of the Joint Committee on Powder Diffraction Standards (JCPDS).

TPR measurements were performed by submitting the catalysts located in a quartz reactor between two quartz wool plugs to a H_2 (13 vol.%)/Ar flow (total flow rate of 50 mL/min) with a heating rate of 15 °C/min from room temperature to 930 °C, at which the catalyst was kept afterwards during 30 min. The H_2 consumption was followed by thermal conductivity catharometric detection.

Microstructural characterization was carried out by TEM on a Topcon 002B working at 200 kV accelerated voltage.

XPS spectra were recorded with pass energy of 20 eV on a ThermoVG Scientific apparatus equipped with an Al Kα source and a hemispherical analyser. The W_{4f} lines were analyzed with a curve fitting procedure according to the Doniach and Sunjic theory [18], using the Shirley background subtraction.

2.3. Catalytic device

The experiments were carried out under H_2 at atmospheric pressure with 100 mg of catalyst powder in a stainless steel micropilot equipped with a quartz reactor (10 and 300 mm of internal diameter and reactor length, respectively). The catalyst bed was thus about 5 mm height, centered in the 70 mm long isothermal zone of the reactor. The catalyst was first pre-reduced (i.e. activated) for 2 h under a 30 mL/min hydrogen flow at temperatures ranging from 200 to 550 °C (heating rate of 15 °C/min), and the reaction was further performed at 200 °C with a H_2 flow rate of 30 mL/min. Hydrocarbon pulses were manually introduced into the H_2 flow using a saturator kept at a constant temperature (−38 °C, obtained using an anisol/liquid nitrogen cooling mixture) leading to a partial pressure of 6.5 Torr of hydrocarbon in flowing H_2. The reactant and reaction products were analyzed on-line by gas chromatography (GC 8000, CEInstruments) equipped with a flame ionization detector. All the unsaturated products were hydrogenated on a separated Pt Adams-based hydrogenator before on-line analysis for easy detection and quantification.

3. Results and discussion

3.1. Catalyst characterization

Fig. 1 shows the XRD pattern of the WO_3/CNT catalysts with WO_3 content ranging from 4 to 30 wt.% and of the fresh CNT support given as reference. On the CNT support, the most intense diffraction peak characteristic of the CNTs at $2\theta = 25.8°$ corresponds to the interlayer scattering of the

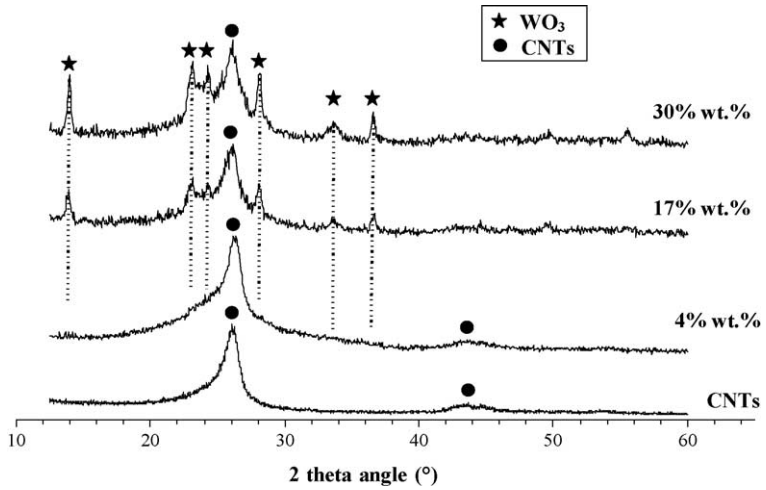

Fig. 1. X-ray diffraction pattern of the WO_3/CNT catalysts. Influence of the tungsten initial content.

basal planes. The presence of WO_3 crystallized domains was only detected for catalysts containing 17 wt.% or more of WO_3, with the peak intensities corresponding to WO_3 (2θ = 14.0, 23.2, 24.5, 28.3, 34.1 and 36.8°) increasing with the W content. The average WO_3 crystallite size derived from the XRD peak broadening was about 20 and 30 nm for the materials containing 17 and 30 wt.% of WO_3, respectively. The WO_3/ZrO_2 material had a specific surface area of 33 m^2/g with a mean WO_3 crystallite size determined by the XRD peak broadening of about 60 nm [16].

TPR profiles of the CNT support of WO_3 (17 wt.%) and WO_3 (30 wt.%)/CNT catalysts are given in Fig. 2, together with that of a commercial bulk WO_3 sample for comparison. One could observe that the CNT support showed no appreciable reduction under hydrogen until 930 °C. Except for the total amount of reducible species, the supported WO_3 (17 wt.%)/CNT and WO_3 (30 wt.%)/CNT catalysts exhibited the same kind of reduction profile with two main reduction steps, the first and smallest one around 628–640 °C and the second one at 680–710 °C. The increase in WO_3 content from 17 to 30 wt.% only led to a slight shift of the reduction steps to higher temperatures. Comparing these profiles with that of bulk WO_3, and according to literature, it could be suggested that the two successive reduction peaks observed on the WO_3/CNT materials correspond to the reduction of bulk-like WO_3 crystallites [19]. These peaks would override the reduction signal of tungstate surface species located at the carbon/oxide interface (if any), which were observed on ZrO_2- and Al_2O_3-supported WO_3 catalysts [15,16]. It should be noted that the total reduction of the bulk WO_3 sample was not achieved before the isotherm step at 930 °C, so that the number of reduction steps, two or three having been observed depending on the reduction conditions as mentioned in the literature, could not be determined. The reduction of the WO_3/ZrO_2 reference showed two main reduction peaks, the first and smallest one at 636 °C like in the case of CNT-based materials and the second one at much higher temperature (780 °C), which was attributed to the final reduction into metallic tungsten [20]. A very small reduction peak located at about 780 °C could also be distinguished on the WO_3 (30 wt.%)/CNT material, thus assigned to the reduction into small amounts of metallic tungsten. The reduction sequence of WO_3 into the metallic state could thus be proposed as follows [21]:

$$WO_3 \rightarrow W_{20}O_{58} \text{ and } W_{20}O_{58} \rightarrow WO_2 \text{ and } WO_2 \rightarrow W$$

We suggest that the reduction sequence reported to form metallic tungsten on the ZrO_2 support was stopped under similar reduction conditions at the WO_2 step using CNTs. The differences in signal intensity, peak position and general profile of the TPR spectra could result from the morphology and/or the chemical nature of the support, whose influence will be discussed in a further section in link with the catalytic behavior.

Fig. 3 shows TEM images of the WO_3 (17 wt.%)/CNT material. Bare CNTs had the usual structure made of ordered graphene sheets oriented parallel with respect to the tube axis with the interlayer spacing of 0.348 nm. TEM images evidenced the exclusive location of the WO_3 domains inside the CNTs, neither WO_3 particles located on the outer walls of CNTs nor non-anchored bulk WO_3 having been observed. Most of the WO_3 was in the nanowire morphology or as 5–10 nm thick films covering the internal surface of CNTs, only very few isolated WO_3 particles having been observed. Such an exclusive location inside CNTs has already been reported during investigations dealing with the decoration of CNTs with palladium metal particles (e.g. 5 wt.%), or with the formation of cobalt ferrite nanowires inside CNTs

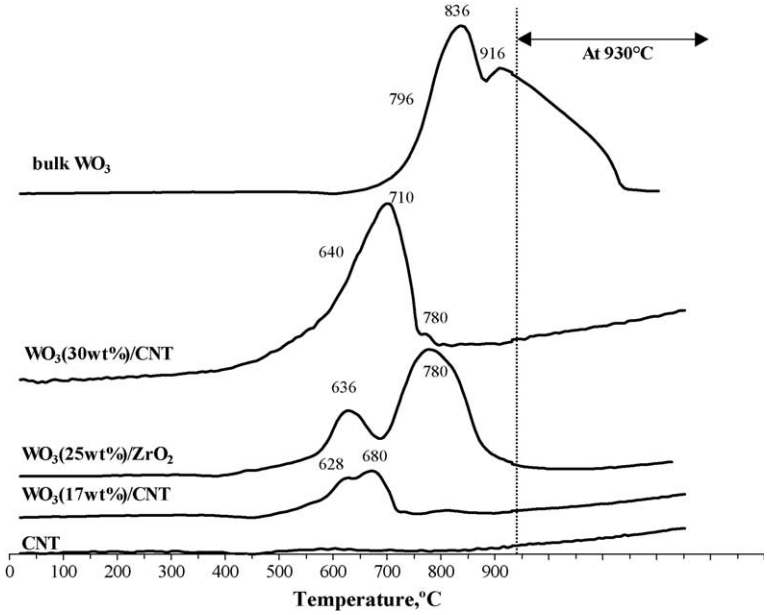

Fig. 2. TPR profiles of WO_3/CNTs, WO_3/ZrO_2 and WO_3 bulk reference.

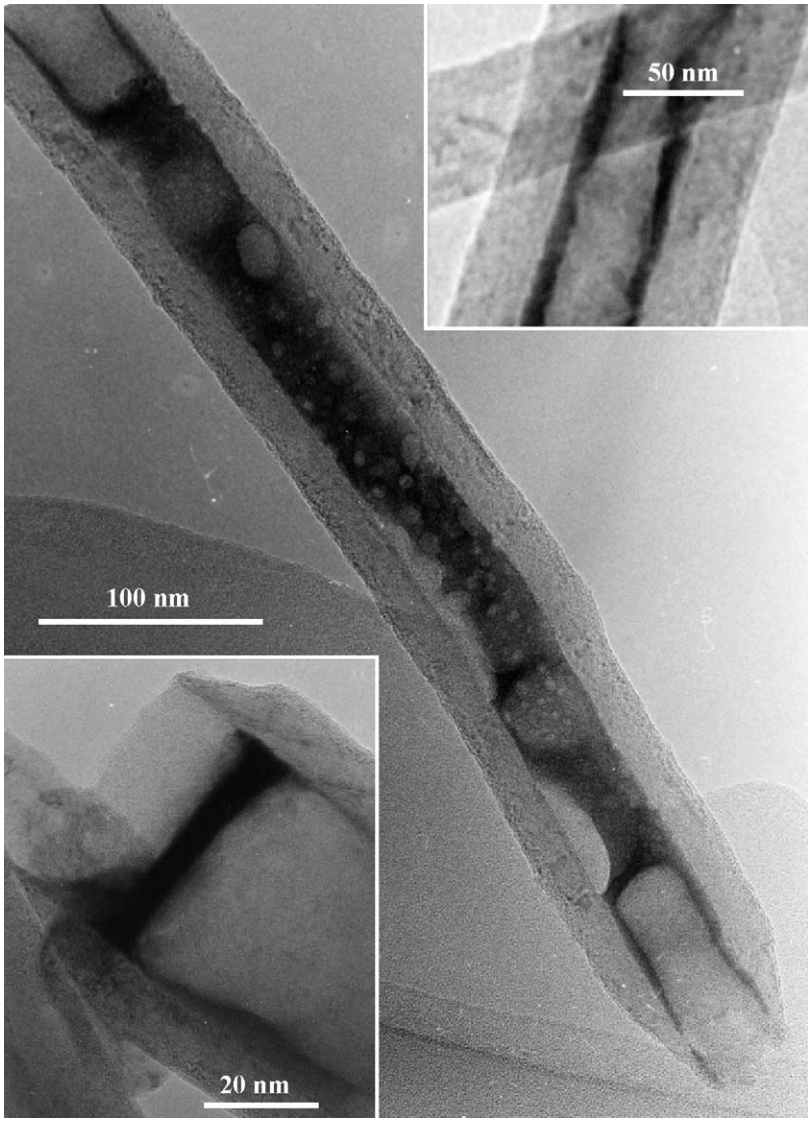

Fig. 3. TEM images of the WO_3 (17 wt.%)/CNT catalyst.

[22,23]. The literature reports that elements and compounds with a surface tension lower than 190 mN/m are efficient for wetting and filling nanotubes [24]. The use of water as solvent with the relatively low surface tension of 72 mN/m led to a totally selective nanotube filling. The inner volume of the MWNTs was completely filled by the paratungstate solution during the impregnation step due to capillary forces. The differences of contrast observed by TEM inside the WO_3 nanowires led to consider the WO_3 nanowires as an aggregation of WO_3 crystallized domains stuck together to form nanowire morphology, in agreement with the 20 nm diameter crystallites measured by XRD, as it has been reported for a CNT-filled $CoFe_2O_4$ material [22].

Fig. 4a and b show, respectively, the W_{4f} and C_{1s} XPS spectra of the WO_3 (17 wt.%)/CNT material as obtained after preparation and calcination at 350 °C for 2 h. The inset in Fig. 4a corresponds to the W_{4f} XPS spectra of the WO_3/ZrO_2 reference. The XPS W_{4f} signal of the WO_3/CNT catalyst (Fig. 4a) could be fitted with one contribution corresponding to the W(VI) oxidation state, located at 35.2 and 37.4 eV for the W_{4f} spin-orbit component. Deconvolution of the W_{4f} XPS spectra of the WO_3/ZrO_2 reference after calcination at 350 °C (insert Fig. 4a) revealed that it could only be fitted with two contributions. The largest one, at 35.2 and 37.4 eV [25], was attributed to W(VI) surface species and the second one at 34.2 and 36.4 eV [26] was assigned to W(V) species. These observations evidenced the importance of the support and especially of the active-phase-support interaction, which was also shown to be extremely different between ZrO_2 and CNTs. Table 1 summarizes the binding energies and the fit parameters used for the W_{4f} components.

Deconvolution of the C_{1s} spectra [27–29] resulted in three contributions, the first one at 284.6 eV, assigned to graphitic sp^2-hybridized carbon, the second one at 286.3 eV, associated to –C–OH phenolic surface groups and the third broad one at 291.2 eV, probably corresponding to a π–π^*

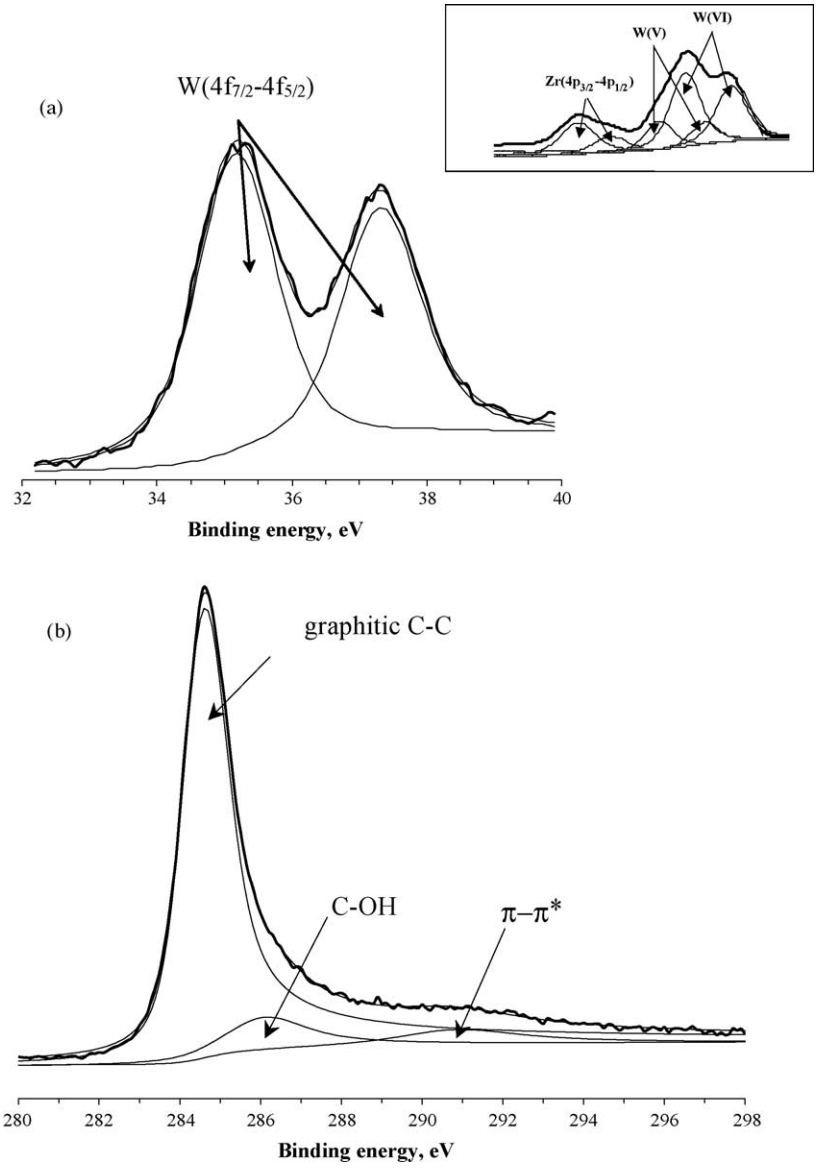

Fig. 4. XPS W_{4f} (a) and C_{1s} (b) spectra of the WO_3 (17 wt.%)/CNT material. The inset (a) corresponds to the XPS W_{4f} spectra of the WO_3 (25 wt.%)/ZrO_2 reference. Sp^2-hybridized carbon C_{1s} peak was taken at 284.6 eV as energy reference.

transition peak (i.e., a surface plasmon peak) due to the metallic properties of sp^2-bound carbon, resulting from the average graphitic nature of CNTs with an extended π-electron conduction band system [29]. The graphitic typical C_{1s} line shape was fitted using an asymmetry, which is a well-known phenomenon occurring in conductive materials [29]. The W/C atomic surface ratio of the WO_3 (17 wt.%)/CNT material determined from the XPS spectra was 0.017. This value was very low compared to the W/Zr ratio (0.22) of the WO_3/ZrO_2 reference, suggesting that a great part of the CNT surface was not uniformly covered with tungsten species. This was in good agreement with the TEM images, which evidenced the exclusive location of the WO_3 domains inside the CNTs, no WO_3 particles having been observed outside of them.

Table 1
Binding energies and full width at half maximum (FWHM) for the W_{4f} 7/2 XPS spectra on the WO_3 (17 wt.%)/CNTs and WO_3 (25 wt.%)/ZrO_2 catalysts

Catalysts	Binding energy of W_{4f} 7/2 (eV)[a]		FWHM of W_{4f} 7/2 (eV)[a]	
	W(VI)	W(V)	W(VI)	W(V)
WO_3 (17 wt.%)/CNTs	35.7	–	0.35	–
WO_3 (25 wt.%)/ZrO_2	35.2	34.2	0.37	0.37

[a] The FWHM was taken identical for both W_{4f} 7/2 and W_{4f} 5/2 components, whereas the spin-orbit constant was set at 2.2 eV and the W_{4f} 5/2 to W_{4f} 7/2 ratio at 0.75.

3.2. Catalytic results

Fig. 5 shows the total specific rate and the isomerization selectivity obtained at 200 °C on the WO_3 (17 wt.%)/CNT

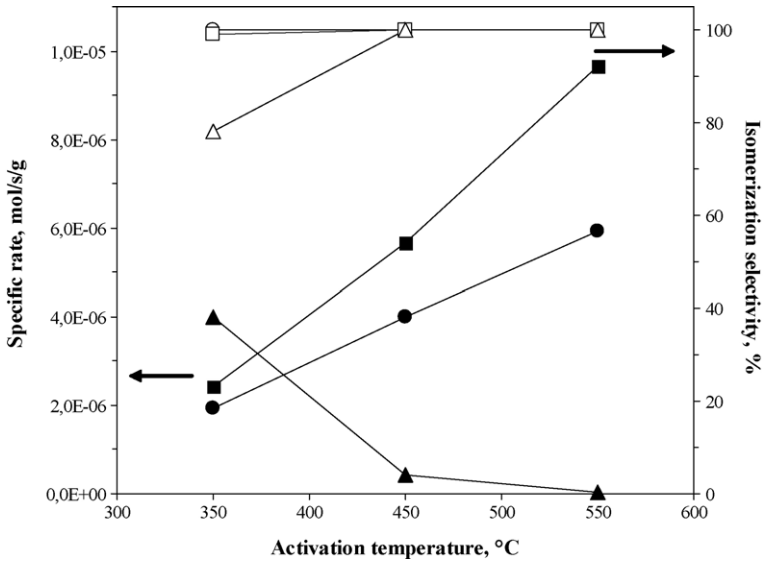

Fig. 5. 4M1Pen reaction at 200 °C on the WO_3 ((■) 17 wt.%; (●) 30 wt.%)/CNTs and the WO_3 (25 wt.%)/ZrO_2 (▲) reference as a function of the reduction temperature. The total specific rates and isomerization selectivities are represented as black and white symbols, respectively. Reactions have been performed in the pulse mode and the results represented correspond to the second pulse of reactant.

and WO_3 (30 wt.%)/CNT catalysts for the 4M1Pen reaction as a function of the activation temperature, ranging from 350 to 550 °C. Catalytic results were compared to that obtained on the WO_3 (25 wt.%)/ZrO_2 reference catalyst. The behavior of the WO_3/CNT catalysts was strongly influenced by the pre-reduction (i.e. activation) conditions. The increase in the activation temperature from 350 to 550 °C yielded the enhancement of the specific rate on both WO_3/CNT catalysts contrarily to the tungstated zirconia sample for which a considerable decrease was observed for activation temperatures higher than 350 °C. It could be pointed out that whatever the activation temperature, only skeletal isomerization occurred and no cracking products were observed on WO_3/CNTs, even at very high conversion level. This interesting behavior differed from what is reported for most of the catalysts used in reforming reactions; indeed, very high isomerization selectivities could only be obtained on WO_3/ZrO_2 catalyst at low conversions. It should be pointed out that the (17 wt.%)/CNT catalyst exhibited the highest efficiency whatever the activation temperature, taking into account both the total specific rate and the isomerization selectivity.

Looking at the catalytic stability between WO_3 (17 wt.%)/CNT and WO_3/ZrO_2 (Fig. 6), the two kinds of materials exhibited completely different behaviors after a series of successive hydrocarbon pulses at 200 °C. It must be noted that the performances obtained on the WO_3 (30 wt.%)/CNT catalyst have not been reported in Fig. 6 because the catalyst displayed the same behavior than the WO_3 (17 wt.%)/CNT sample. Whatever the pre-reduction temperature, the WO_3/CNT catalysts were very stable after successive reactant pulses and kept an isomerization selectivity of 100% contrarily to the WO_3/ZrO_2 catalyst, which was subject to strong deactivation. Indeed, the catalytic activity of the tungstated zirconia was stable for an activation temperature of 350 °C, but rapidly deactivated at 450 °C and even more rapidly at 550 °C, although the initial activity after activation at 550 °C was already very low. It has been already observed on some WO_3-supported systems like WO_3/ZrO_2 [20] and WO_3/Al_2O_3 [15] that deactivation of the catalyst for hydrocarbon reactions was due to the formation of metallic tungsten.

In this study, it has been evidenced that on WO_3/CNT materials, the formation of metallic tungsten was hindered explaining the absence of any observable deactivation phenomenon. It is admitted that on supports like Al_2O_3 or ZrO_2, the complete reduction can be achieved at moderate

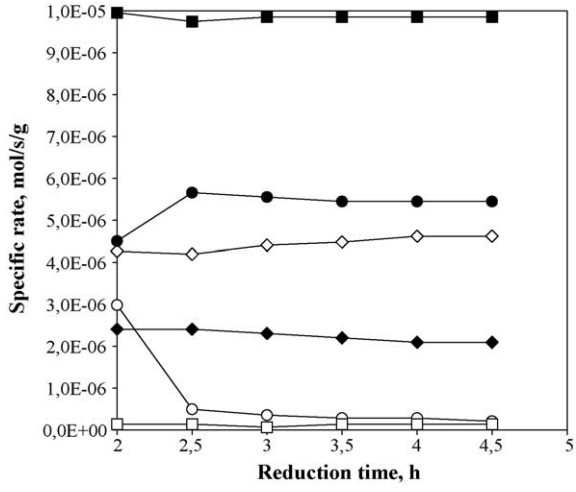

Fig. 6. Evolution of 4M1Pen reaction at 200 °C on WO_3 (17 wt.%)/CNT (full symbols) and WO_3 (25 wt.%)/ZrO_2 (empty symbols) as a function of successive hydrocarbon pulses after 2 h activation at 350 (◆, ◇), 450 (●, ○) and 550 °C (■, □).

temperature only if WO_3 crystallites behaving as bulk (or bulk-like) WO_3 are present [15,16,25,30]. Consequently, the total reduction of bulk-like WO_3 crystallite domains located inside CNTs should have been easily possible at reduction temperature of 550 °C, as their mean crystallite diameter was close to that of WO_3 present on the WO_3/ZrO_2 reference. In fact, the reducibility of WO_3 into metallic tungsten was very limited, pointing out an effect of the CNT support. Thus, hindering the WO_3 reducibility inside CNTs compared to on a ZrO_2 support could explained both improved isomerization performances and stability of CNT-based catalysts relatively to ZrO_2, for which the metallic state of tungsten first led to extensive cracking, and further resulting in the catalyst poisoning. The lower specific rate obtained on the highly loaded CNT-based catalyst compared to the 17 wt.% one could be explained by a worse dispersion of WO_3. This had probably decreased the real amount of WO_3 taking part to the reaction.

It could be proposed that the limited reduction process inside CNTs could be explained (i) by the reduced accessibility to WO_3 nanowires rather than by a confinement effect in the case of H_2 molecules and/or (ii) by a specific WO_3–carbon inner walls interaction when WO_3 was present as thin films.

However, the hypothesis of a confinement effect of hydrocarbons inside CNTs, put forward for other molecules [23], could not be excluded and should be discussed in a further paper.

4. Conclusion

This study clearly evidenced the positive role of carbon nanotubes when used as a support for WO_3 in order to prevent a complete reduction into metallic tungsten, thus limiting the deactivation of the catalyst, as usually observed on ‘‘classical’’ supports at moderate temperatures. Some complementary studies using reactants with longer carbon atom chains and working at higher pressure are now in course to confirm if this confinement effect is also valid on the catalytic activity. Furthermore, the surface state of tungsten on carbon nanotubes as a function of the reduction temperature is currently under investigation by in situ XPS.

The WO_3/CNT materials exhibited monofunctional acidic skeletal isomerization properties with very high (100%) skeletal isomerization selectivities even at high conversion levels, confirmed by the fact that they are only active for olefin reactions but exhibit no activity toward saturated reactants. Determination of the optimal tungsten content located inside carbon nanotubes is currently under investigation in order to increase the WO_3 dispersion, i.e., for improving the content of WO_3 really involved in the reaction. Work is ongoing to make them active in the same way for saturated hydrocarbon skeletal isomerization with the addition of metallic properties via the introduction of Pt exclusively inside the carbon nanotubes to lead to a bifunctional Pt–WO_3/CNT catalyst.

Acknowledgments

P. Bernhardt (LMSPC) is acknowledged for helping during XPS analysis. The authors would like to thank S. Joulie (IPCMS, UMR 7504 CNRS) and S. Libs (LMSPC) for having performed TEM and TPR characterization.

References

[1] E. Iglesia, D.G. Barton, S.L. Soled, S. Miseo, J. Baumgartner, W.E. Gates, G.A. Fuentes, G.D. Meitzner, in: Proceedings of the 11th International Congress of Catalysis, Baltimore 1996, Stud. Surf. Sci. Catal. 101 (1996) 533.
[2] X. Song, A. Sayari, Catal. Rev. -Sci. Eng. 38 (1996) 329.
[3] D.A. Ward, E.I. Ko, J. Catal. 150 (1994) 18.
[4] M. Hino, K. Arata, J. Chem. Soc., Chem. Commun. (1987) 1259.
[5] G. Ramis, G. Busca, Appl. Catal. A 107 (2) (1994) 249.
[6] V.M. Benitez, N.S. Figoli, Catal. Commun. 3 (2002) 487.
[7] J. Dowody, M. Skoylundh, E. Fridell, J. Mol. Catal. A 209 (2004) 215.
[8] L.L. Murrell, N.C. Dispenziere Jr., Catal. Lett. 4 (1990) 235.
[9] V.M. Benitez, C.A. Querini, N.S. Figoli, Appl. Catal. A 252 (2) (2003) 427.
[10] V.C.F. Holm, G.C. Bailey, US Patent No. 3032599, 1962.
[11] C. Moreno-Castilla, F.J. Maldonado-Hodar, J. Rivera-Utilla, E. Rodrigues-Castellon, Appl. Catal. A 183 (1999) 345.
[12] M.A. Alvarez-Merino, F. Carraso-Marin, C. Moreno-Castilla, J. Catal. 192 (2000) 374.
[13] A.F. Pérez-Cadenas, C. Moreno-Castilla, F.J. Maldonado-Hodar, J.L.G. Fierro, J. Catal. 217 (2003) 30.
[14] L.R. Radovic, F. Rodriguez-Reinoso, in: P.A. Thrower, M. Deckker (Eds.), Chemistry and Physics of Carbon, vol. 25, Dekker, New York, 1997, p. 243.
[15] V. Logie, G. Maire, D. Michel, J.L. Vignes, J. Catal. 188 (1999) 90.
[16] F. Di Gregorio, V. Keller, J. Catal. 225 (2004) 45.
[17] P. Serp, M. Corria, P. Kalck, Appl. Catal. A 253 (2003) 337.
[18] S. Doniach, M. Sunjic, J. Phys. C 3 (1970) 285.
[19] D.G. Barton, S.L. Soled, G.D. Meitzner, G.A. Fuentes, E. Iglesia, J. Catal. 181 (1999) 57.
[20] F. Di Gregorio, Ph.D Dissertation, Louis Pasteur University of Strasbourg, France, 2003.
[21] W.D. Schubert, Int. Refract. Hard Met. 9 (1990) 178.
[22] C. Pham-Huu, N. Keller, C. Estournès, G. Ehret, J.M. Grenèche, M.J. Ledoux, Phys. Chem. Chem. Phys. 5 (2003) 3716.
[23] J.M. Nhut, P. Nguyen, C. Pham-Huu, N. Keller, M.J. Ledoux, Catal. Today 91–92 (2004) 91.
[24] D. Ugarte, A. Châtelain, W.A. de Heer, Science 274 (1996) 1897.
[25] M. Valigi, D. Gazzoli, I. Pettiti, G. Mattei, S. Colonna, D. De Rossi, G. Ferraris, Appl. Catal. 231 (2002) 159.
[26] E. Salje, A.F. Carley, M.W. Roberts, J. Solid. State Chem. 29 (1979) 237.
[27] U. Zielke, K.J. Hütger, W.P. Hoffman, Carbon 34 (1996) 983.
[28] Z.R. Yue, W. Jiang, L. Wang, H. Toghiani, S.D. Gardner, Carbon 37 (1999) 1785.
[29] H. Estrade-Szwarckopf, Carbon 42 (2004) 1713.
[30] S.R. Vaudagna, S.A. Canavese, R.A. Comelli, N.S. Figoli, Appl. Catal. A 168 (1998) 93.